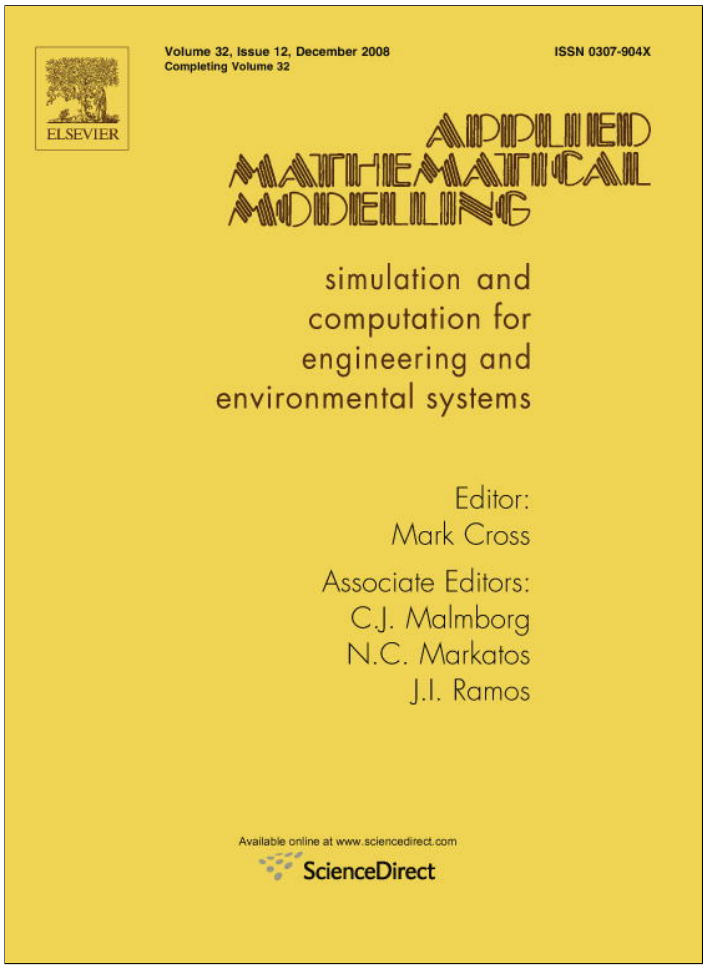

Available online at www.sciencedirect.com
ScienceDirect
Applied Mathematical Modelling 32 (2008) 2925–2935
APPLIED MATHEMATICAL MODELLING
www.elsevier.com/locate/apm

Closed-form solutions for a mode III radial matrix crack penetrating a circular inhomogeneity

X. Wang [a,b,*], E. Pan [a,b], W.J. Feng [c]

[a] Department of Civil Engineering, University of Akron, Akron, OH 44325-3905, United States
[b] Department of Applied Mathematics, University of Akron, Akron, OH 44325-3905, United States
[c] Department of Engineering Mechanics, Shijiazhuang Railway Institute, Shijiazhuang 050043, PR China

Received 22 February 2007; received in revised form 23 September 2007; accepted 10 October 2007
Available online 17 October 2007

Abstract

In this research we address in detail a mode III radial matrix crack penetrating a circular inhomogeneity. One tip of the radial crack lies in the matrix, while the other tip of the radial crack lies in the circular inhomogeneity. In addition the two tips of the crack are mutually image points (or inverse points) with respect to the circular inhomogeneity-matrix interface. First we conformally map the crack onto a unit circle C_a in the new ζ-plane. Meanwhile the inhomogeneity-matrix interface is mapped onto C_b, a part of another circle in the ζ-plane. In addition C_a and C_b intersect at a vertex angle $\pi/2$. By using the method of image in the ζ-plane, closed-form solutions in terms of elementary functions are derived for three loading cases: (1) remote uniform antiplane shearing; (2) a screw dislocation located in the unbounded matrix; and (3) a radial Zener–Stroh crack.

Keywords: Closed-form solution; Crack; Inhomogeneity; Conformal mapping; Image method

1. Introduction

When addressing matrix or fiber cracking problems in fiber-reinforced composite, it is often needed to resort to numerical methods (for example numerically solving the resulting singular integral equations) to arrive at those physical quantities of interest such as stress intensity factors and crack opening displacement [1–7]. It is extremely desirable to obtain closed-form solutions in terms of elementary functions even under some special conditions for crack problems in fiber-reinforced composite since the fact that the physical quantities of interest can be extracted from the obtained solutions conveniently, and that the closed-form solutions can be used to validate various numerical methods. The aim of this research is to pursue such a solution.

* Corresponding author. Address: Department of Civil Engineering, University of Akron, Akron, OH 44325-3905, United States. Tel.: +1 330 972 2457; fax: +1 330 972 6020.
E-mail addresses: xuwang@uakron.edu (X. Wang), pan2@uakron.edu (E. Pan), fengwenjie2005@hotmail.com (W.J. Feng).

0307-904X/$ - see front matter
doi:10.1016/j.apm.2007.10.008

In this study we consider a radial matrix crack penetrating a circular elastic inhomogeneity under antiplane shear deformations. In our discussion, one tip of the radial crack lies in the matrix, while another tip is lodged in the inhomogeneity. We confine our attention to the special situation in which the two tips of the crack are mutually image points (or inverse points) with respect to the circular interface between the inhomogeneity and the surrounding matrix. First the conformal mapping method is applied to map the crack onto a unit circle in the new ζ-plane. It is proved that under such a conformal mapping, the inhomogeneity-matrix interface can be mapping onto a portion of another circle. In addition the intersection angle of the two circles in the ζ-plane is $\pi/2$. Here it is stressed that the resulting boundary value problem in the new ζ-plane is *similar* to the electrostatic problem of a circular conductor partially merged in a dielectric cylinder with a dielectric constant different from that of the surrounding host medium, which was recently discussed by Palaniappan [8]. By using Kelvin's inverse (or method of image) [9–12] together with shift and reflection properties of harmonic functions, he analytically solved the exterior boundary value problem. Here we can conveniently adapt Palaniappan's result to our investigation. Closed-form solutions are derived for three cases: (1) the two-phase composite is subjected to remote uniform shearing; (2) a screw dislocation is located in the matrix; (3) the radial crack is a Zener–Stroh crack.

2. The elastostatic problem and conformal mapping

As shown in Fig. 1, a circular inhomogeneity with shear modulus μ_1 is embedded in an unbounded matrix with another shear modulus μ_2. The inhomogeneity and the surrounding matrix form a perfect interface L across which tractions and displacements are continuous. A radial matrix crack enters the inhomogeneity. Traction-free conditions are satisfied on the crack surface. The origin of the Cartesian coordinate system (x, y) is chosen at the centre of the crack, with the crack lying on the x-axis. The half-length of the crack is unit 1. In this investigation we consider a special situation in which the circular interface L intersects the real x-axis at the two points $(1/c, 0)$ and $(c, 0)$, $(c > 1)$. In this situation the left and right tips of the crack are just mutually image points with respect to the circle L. It is apparent that the radius of the circle L is $\frac{1}{2}(c - \frac{1}{c})$, and the center of the circle L is at $(\frac{1}{2}(c + \frac{1}{c}), 0)$. Three loading cases will be discussed: (1) the two-phase composite is subjected to remote uniform antiplane shearing σ_{zy}^{∞}; (2) a screw dislocation with Burgers vector b_z is located at $z = z_0$ $(z = x + \mathrm{i}y)$ in the matrix; (3) the radial crack is a Zener–Stroh crack with a total Burgers vector b_z. The antiplane displacement w and the two stress components σ_{zy} and σ_{zx} can be expressed in terms of a single analytic function $f(z)$ as [13]

$$\begin{aligned} w &= \mathrm{Im}\{f(z)\}, \\ \sigma_{zy} + \mathrm{i}\sigma_{zx} &= \mu f'(z). \end{aligned} \tag{1}$$

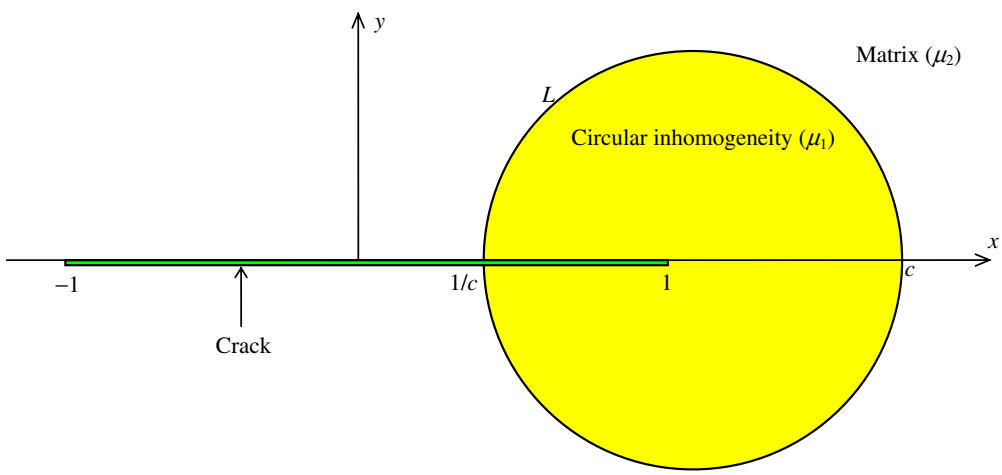

Fig. 1. A mode-III radial matrix crack penetrates a circular inhomogeneity.

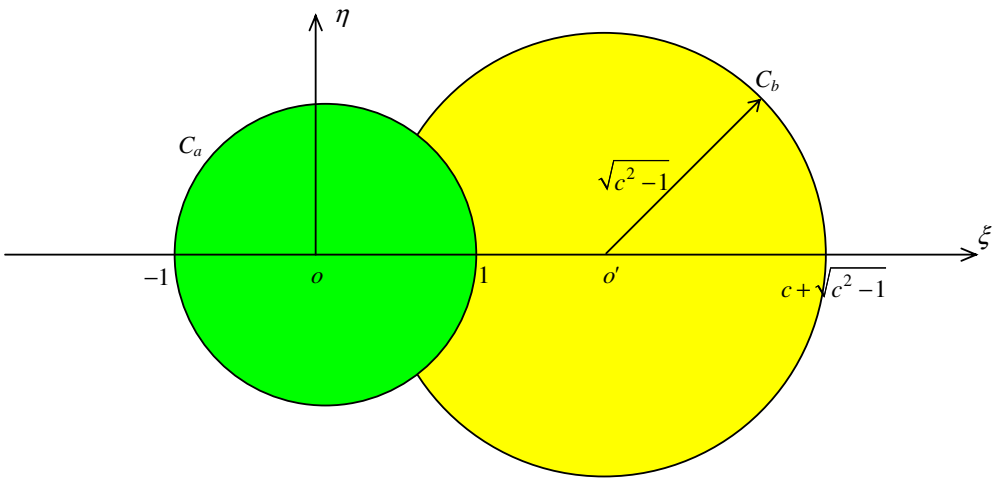

Fig. 2. The mapped geometry in the ζ-plane.

We first introduce the following conformal mapping function:

$$z = m(\zeta) = \frac{1}{2}\left(\zeta + \frac{1}{\zeta}\right), \tag{2}$$

which maps the exterior of the crack onto the exterior of a unit circle C_a in the ζ-plane ($\zeta = \xi + i\eta$), as shown in Fig. 2. Meanwhile it is proved in the Appendix that the interface L is mapped onto C_b, which is part of another circle of radius $\sqrt{c^2-1}$ in the ζ-plane. The two circles C_a and C_b overlap at a contact angle $\pi/2$ due to the property of conformal mapping and the fact that in the physical z-plane the crack and the circular interface L intersect at an angle $\pi/2$. The mapping point of the centre of the circle L is still the centre of C_b. The distance between the centres of C_a and C_b is c. Our task below is to determine the analytic function $f_1(\zeta)$ defined in the inhomogeneity and $f_2(\zeta)$ defined in the matrix. Here for convenience we write $f_i(z) = f_i(m(\zeta)) = f_i(\zeta)$, $i = 1, 2$. We find that the resulting boundary value problem in the new ζ-plane is very similar to the electrostatic problem recently discussed by Palaniappan [8] of a 2D snowman type of an object with a conducting cylinder partially protruded into a dielectric cylinder with a dielectric constant different from that of the surrounding host medium. It shall be mentioned that the traction-free boundary condition on the crack surface discussed here is of Neumann-type; while the zero-potential on the conductor surface discussed by Palaniappan [8] is of Dirichlet-type. In the next section we will derive closed form solutions in the ζ-plane by using the method of image (or continuously using analytic continuation on C_a and C_b).

3. General solutions

3.1. Remote uniform shearing

When the two-phase composite is only subjected to remote uniform shearing σ_{zy}^{∞}, by using the method of image [8] and also noticing the conformal mapping Eq. (2), the two analytic functions $f_1(\zeta)$ defined in the inhomogeneity and $f_2(\zeta)$ defined in the unbounded matrix can be expressed in closed-form as

$$\begin{aligned} f_1(\zeta) &= \frac{\sigma_{zy}^{\infty}\Gamma}{2\mu_2}\left(\zeta - \frac{1}{\zeta}\right), \\ f_2(\zeta) &= \frac{\sigma_{zy}^{\infty}}{2\mu_2}(\zeta^2 - 1)\left[\frac{1}{\zeta} + \frac{(c^2-1)(1-\Gamma)}{(\zeta - c)(c\zeta - 1)}\right], \end{aligned} \tag{3}$$

where $\Gamma = \frac{2\mu_2}{\mu_1+\mu_2}$, and $\zeta = m^{-1}(z) = z + \sqrt{z^2-1}$ with a branch cut on the crack surface. Consequently the full field expressions of the antiplane displacement is given by

$$w = \frac{\sigma_{zy}^{\infty}\Gamma}{2\mu_2}\mathrm{Im}\left\{\zeta - \frac{1}{\zeta}\right\} \tag{4}$$

inside the circular inhomogeneity, and

$$w = \frac{\sigma_{zy}^{\infty}}{2\mu_2}\mathrm{Im}\left\{(\zeta^2 - 1)\left[\frac{1}{\zeta} + \frac{(c^2-1)(1-\Gamma)}{(\zeta - c)(c\zeta - 1)}\right]\right\}, \tag{5}$$

within the unbounded matrix. Fig. 3 shows the contour plots of out-of plane displacement with $c = 5$ and $\mu_1/\mu_2 = 2$ (the inhomogeneity is stiffer than the matrix). We observe that the displacement is continuous across the perfect interface L, while the displacement undergoes a jump across the radial crack.

It follows from Eq. (1) $_2$ that the stress field is obtained by differentiating Eq. (3) as

$$\sigma_{zy} + \mathrm{i}\sigma_{zx} = \sigma_{zy}^{\infty}(2 - \Gamma)\frac{\zeta^2 + 1}{\zeta^2 - 1} \tag{6}$$

inside the circular inhomogeneity, and

$$\sigma_{zy} + \mathrm{i}\sigma_{zx} = \frac{\sigma_{zy}^{\infty}}{\zeta^2 - 1}\left[\zeta^2 + 1 + (\Gamma - 1)(c^2 - 1)\left(\frac{\zeta^2}{(\zeta - c)^2} + \frac{\zeta^2}{(c\zeta - 1)^2}\right)\right], \tag{7}$$

within the matrix. Apparently due to the interference of the crack, the stress field inside the inhomogeneity is no longer uniform. We can use the average stresses in the inhomogeneity, which are just the stresses at the centre of the circular inhomogeneity in view of the fact that the average value of a harmonic function within any circular inhomogeneity is exactly equal to its value at the centre of the circular inhomogeneity [14], to measure the overall stress level within the inhomogeneity. It follows from Eq. (6) that the average stresses within the inhomogeneity, which are also the stresses at the centre of the circular inhomogeneity, can be evaluated to be

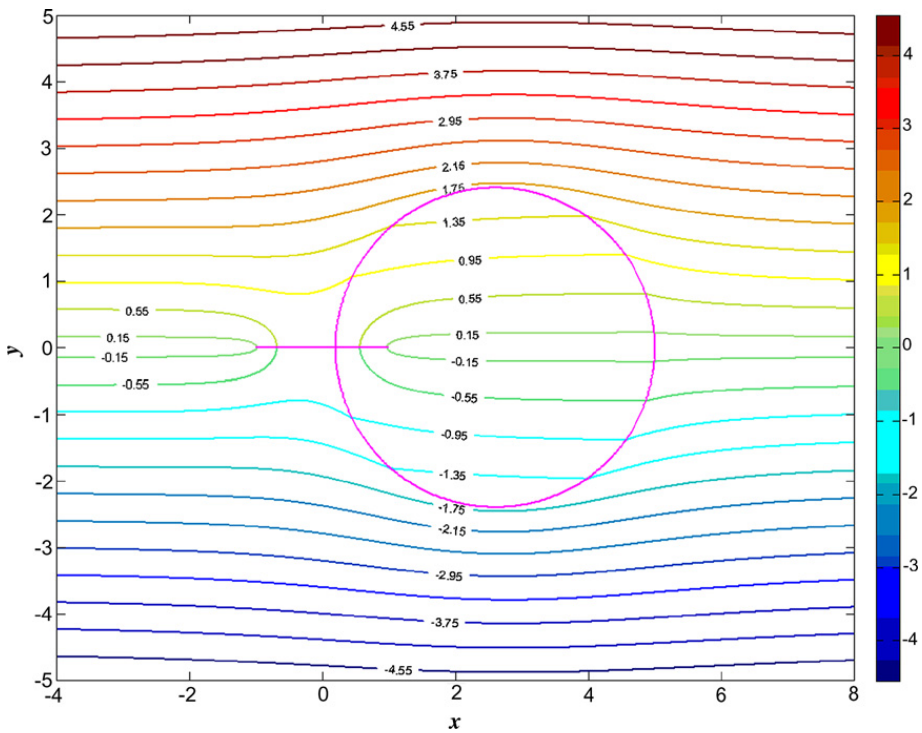

Fig. 3. Contours of normalized out-of plane displacement $\tilde{w} = \frac{\mu_2}{\sigma_{zy}^{\infty}}w$ with $c = 5$ and $\mu_1/\mu_2 = 2$ when the matrix is subjected to remote uniform stress σ_{zy}^{∞}.

$$\bar{\sigma}_{zy} = \sigma_{zy}^{\infty}(2-\Gamma)\frac{c^2+1}{c^2-1}, \quad \bar{\sigma}_{zx} = 0, \tag{8}$$

where over bar means the average. Remember that in the absence of the radial crack, the average stresses within the inhomogeneity under the same loading are [15]

$$\bar{\sigma}_{zy} = \sigma_{zy}^{\infty}(2-\Gamma), \quad \bar{\sigma}_{zx} = 0. \tag{9}$$

Comparing Eq. (8) with Eq. (9), we observe that the average stress within a cracked inhomogeneity is *higher* than that within the same circular inhomogeneity with no crack.

Fig. 4 shows the contours of the stress component σ_{zy} in the two-phase composite with $c = 5$ and $\mu_1/\mu_2 = 2$. From this figure we can clearly see how the existence of the crack disturbs the stress field inside the inhomogeneity. On the other hand the stress component σ_{zy} is in general discontinuous across the interface L due to the mismatch in stiffness between the inhomogeneity and matrix.

From the expressions of the stress field, we can arrive at the stress intensity factors (SIFs) on the two tips of the crack as [16,17]

$$\begin{aligned} K_{\mathrm{III}}^{\mathrm{L}} &= \lim_{z\to -1}\sqrt{2\pi|z+1|}\sigma_{zy} = \sqrt{\pi}\sigma_{zy}^{\infty}\left[1+(\Gamma-1)\frac{c-1}{c+1}\right], \\ K_{\mathrm{III}}^{\mathrm{R}} &= \lim_{z\to 1}\sqrt{2\pi|z-1|}\sigma_{zy} = \sqrt{\pi}(2-\Gamma)\sigma_{zy}^{\infty}, \end{aligned} \tag{10}$$

where the superscript 'L' indicates the SIF on the left crack tip, while the superscript 'R' indicates the SIF on the right crack tip.

When the inhomogeneity is stiffer than the matrix, i.e., $\Gamma < 1$, then we have $K_{\mathrm{III}}^{\mathrm{R}} > \sqrt{\pi}\sigma_{zy}^{\infty} > K_{\mathrm{III}}^{\mathrm{L}}$; when the inhomogeneity is softer than the matrix, i.e., $\Gamma > 1$, then we have $K_{\mathrm{III}}^{\mathrm{R}} < \sqrt{\pi}\sigma_{zy}^{\infty} < K_{\mathrm{III}}^{\mathrm{L}}$. Here $\sqrt{\pi}\sigma_{zy}^{\infty}$ is the SIF for a Griffith crack of half-length 1 in a homogeneous material. The crack face displacement jump $\Delta w = w(x,0^+) - w(x,0^-)$ is given by

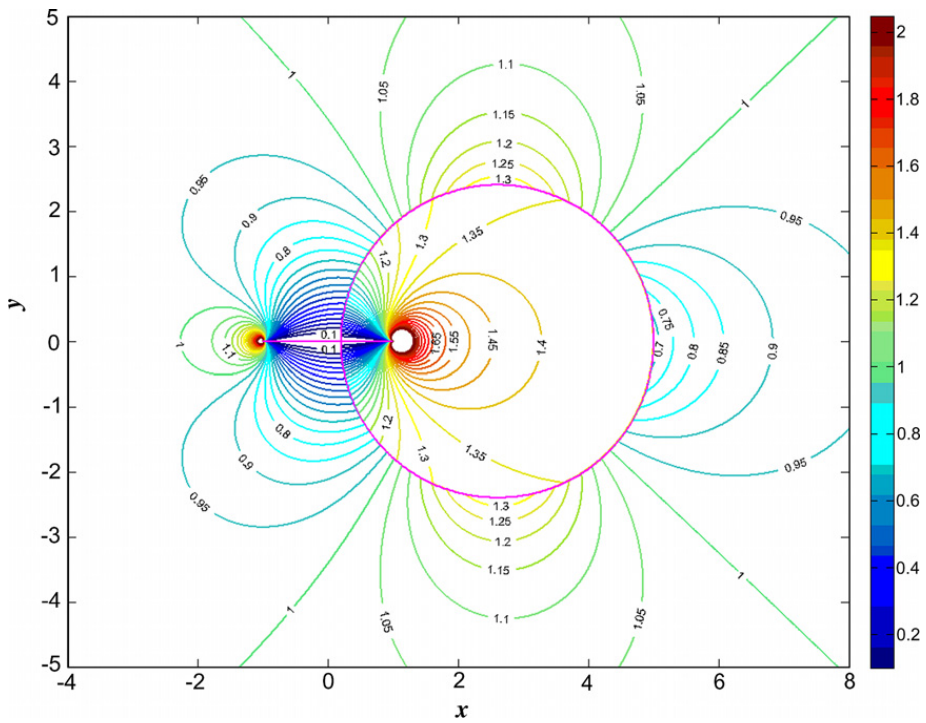

Fig. 4. Contours of the normalized stress component $\tilde{\sigma}_{zy} = \frac{\sigma_{zy}}{\sigma_{zy}^{\infty}}$ with $c = 5$ and $\mu_1/\mu_2 = 2$ when the matrix is subjected to remote uniform stress σ_{zy}^{∞}.

$$\Delta\tilde{w} = \frac{\mu_2}{\sigma_{zy}^{\infty}}\Delta w = \begin{cases} 2\sqrt{1-x^2}\left[1+\frac{(c^2-1)(1-\Gamma)}{2cx-1-c^2}\right], & -1 \leqslant x \leqslant \frac{1}{c}, \\ 2\Gamma\sqrt{1-x^2}, & \frac{1}{c} \leqslant x \leqslant 1. \end{cases} \tag{11}$$

We demonstrate in Fig. 5 the normalized crack face displacement jump $\Delta\tilde{w}$ for different values of μ_1/μ_2 with $c = 5$. In this figure the red dashed line is the trace of the calculated maximum value of $\Delta\tilde{w}$. It is observed that the maximum value of $\Delta\tilde{w}$ always occurs in the matrix part of the crack no matter whether the inhomogeneity is stiffer or softer than the matrix, and the location of the maximum value of $\Delta\tilde{w}$ moves toward the interface L as the ratio μ_1/μ_2 decreases.

3.2. A screw dislocation in the matrix

In this subsection we consider the situation in which a screw dislocation with Burgers vector b_z is located at $z_0 = x_0 + \mathrm{i}y_0$ in the matrix. By using the method of image [8], the two analytic functions $f_1(\zeta)$ defined in the inhomogeneity and $f_2(\zeta)$ defined in the unbounded matrix can be expressed in closed-form as

$$\begin{aligned} f_1(\zeta) &= \Gamma\frac{b_z}{2\pi}\left[\ln(\zeta-e) - \ln\left(\zeta-\frac{1}{\bar{e}}\right) + \ln\zeta\right], \\ f_2(\zeta) &= \frac{b_z}{2\pi}\left[\ln(\zeta-e) - \ln\left(\zeta-\frac{1}{\bar{e}}\right) + \ln\zeta\right] \\ &\quad + (1-\Gamma)\frac{b_z}{2\pi}\left[\ln\left(\zeta-\frac{\bar{e}c-1}{\bar{e}-c}\right) - \ln(\zeta-\frac{e-c}{ec-1}) + \ln\left(\zeta-\frac{1}{c}\right) - \ln(\zeta-c)\right], \end{aligned} \tag{12}$$

where $e = m^{-1}(z_0) = z_0 + \sqrt{z_0^2-1}$.

By differentiating Eq. (12), we can obtain the stress field induced by the screw dislocation located in the matrix as

$$\sigma_{zy} + \mathrm{i}\sigma_{zx} = \frac{\mu_1\Gamma b_z}{\pi(\zeta^2-1)}\left(\frac{\zeta^2}{\zeta-e} - \frac{\zeta}{\bar{e}\zeta-1}\right) \tag{13}$$

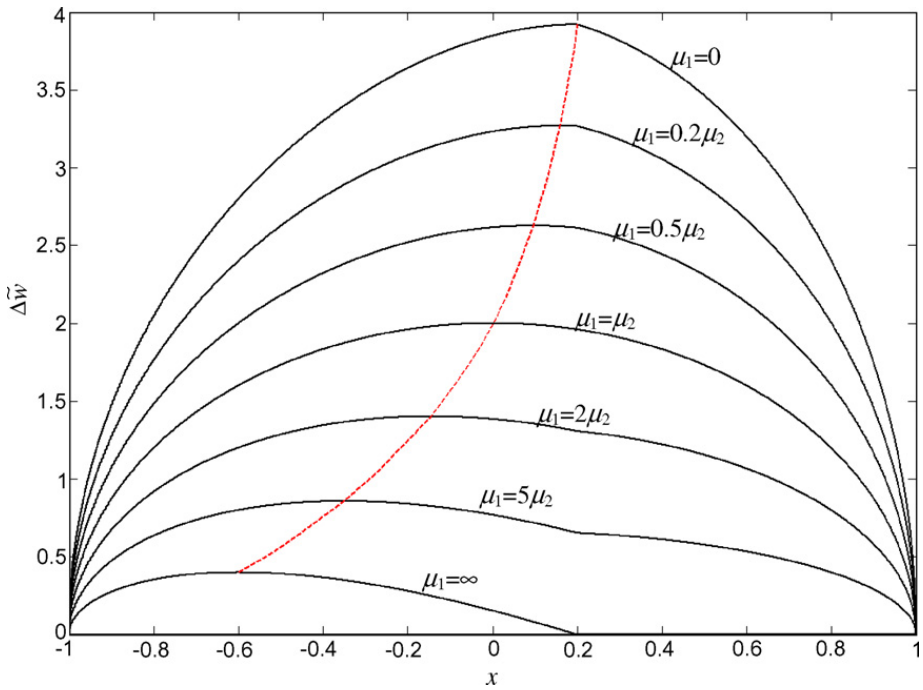

Fig. 5. The normalized crack face displacement jump $\Delta\tilde{w} = \frac{\mu_2}{\sigma_{zy}^{\infty}}\Delta w$ for different values of $\mu_1/\mu_2$with $c = 5$ when the matrix is subjected to remote uniform stress σ_{zy}^{∞}. The dashed line is the trace of the maximum value of Δw.

inside the inhomogeneity, and

$$\sigma_{zy} + \mathrm{i}\sigma_{zx} = \frac{\mu_2 b_z}{\pi(\zeta^2 - 1)}\left(\frac{\zeta^2}{\zeta - e} - \frac{\zeta}{\bar{e}\zeta - 1}\right) + \frac{\mu_2(1-\Gamma)(c^2-1)b_z\zeta^2}{\pi(\zeta^2-1)}\left[\frac{|e|^2 - 1}{[(\bar{e}-c)\zeta - (\bar{e}c-1)][(ec-1)\zeta - (e-c)]} - \frac{1}{(\zeta - c)(c\zeta - 1)}\right] \tag{14}$$

in the matrix. Fig. 6 demonstrates the contour plots of the stress component σ_{zx} induced by a screw dislocation at $(-1.1, 0)$ on the negative x-axis in the matrix with $c = 5$ and $\mu_1/\mu_2 = 2$. Once again we observe that due to the mismatch in shear modulus between the inhomogeneity and matrix, σ_{zx} is not continuous across the interface L.

The SIFs on the two cracks tips due to the screw dislocation are

$$\begin{aligned} K_{\mathrm{III}}^{\mathrm{L}} &= \lim_{z\to -1}\sqrt{2\pi|z+1|}\sigma_{zy} = -\frac{\mu_2 b_z}{\sqrt{\pi}} Re\left\{\frac{1}{1+e}\right\} + \frac{\mu_2(\Gamma-1)(c-1)b_z}{2\sqrt{\pi}(c+1)}\left[1 + \frac{1-|e|^2}{(\bar{e}-1)(e-1)}\right], \\ K_{\mathrm{III}}^{\mathrm{R}} &= \lim_{z\to 1}\sqrt{2\pi|z-1|}\sigma_{zy} = \frac{\mu_1 \Gamma b_z}{\sqrt{\pi}} Re\left\{\frac{1}{1-e}\right\}. \end{aligned} \tag{15}$$

Here it is of interest to investigate $K_{\mathrm{III}}^{\mathrm{L}}$ in more detail. The results show that there exists a curve for the position (x_0, y_0) of the screw dislocation on which $K_{\mathrm{III}}^{\mathrm{L}} = 0$. On the left hand side of the curve, the screw dislocation has an antishielding effect on the left crack tip ($K_{\mathrm{III}}^{\mathrm{L}} > 0$); while on the right hand side of the curve the screw dislocation has a shielding effect on the left crack tip ($K_{\mathrm{III}}^{\mathrm{L}} < 0$). We demonstrate in Fig. 7 the variations of the curve for different values of the ratio μ_1/μ_2 with $c = 5$. When the inhomogeneity becomes stiffer (i.e., μ_1/μ_2 increases), the antishielding region shrinks while the shielding region enlarges.

By substituting the stress field acting on the screw dislocation (Eq. (14) subtracting the stress due to the dislocation itself) into the Peach–Koehler formula [17–19], the image force on the screw dislocation due to its interaction with the crack and the inhomogeneity is

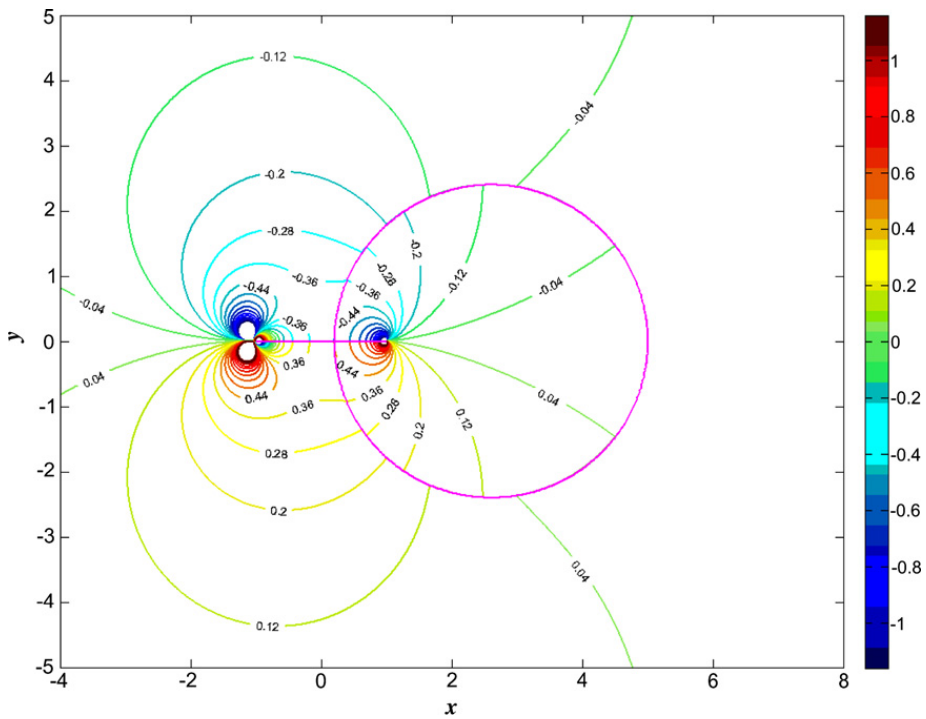

Fig. 6. Contours of the normalized stress component $\tilde{\sigma}_{zx} = \frac{\pi\sigma_{zx}}{\mu_2 b_z}$ induced by a screw dislocation located at $(-1.1, 0)$ on the negative x-axis in the matrix with $c = 5$ and $\mu_1/\mu_2 = 2$.

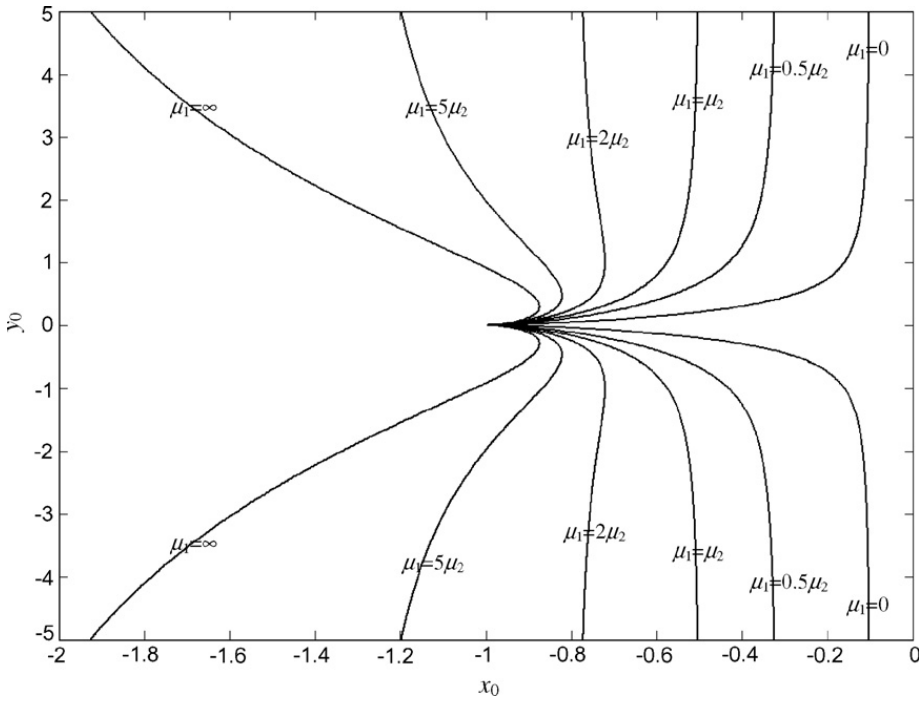

Fig. 7. The variations of the curve on which $K_{\mathrm{III}}^{\mathrm{L}} = 0$ for different values of the ratio μ_1/μ_2 with $c = 5$.

$$F_x - iF_y = \frac{\mu_2 b_z^2 e}{\pi(1-e^2)}\left(\frac{1}{e^2-1} + \frac{1}{|e|^2-1}\right) + \frac{\mu_2(1-\Gamma)(c^2-1)b_z^2 e^2}{\pi(e^2-1)}\left[\frac{|e|^2-1}{[|e|^2-(e+\bar{e})c+1][(e^2+1)c-2e]} - \frac{1}{(e-c)(ec-1)}\right], \tag{16}$$

where F_x and F_y are respectively the components of the image force along the x and y directions. Our calculations also show that under some conditions there exist stable or unstable equilibrium positions for the screw dislocation.

3.3. A radial Zener–Stroh crack

In the previous two subsections the radial crack studied is in fact the well-known Griffith crack. In this subsection we consider the case in which the radial crack $[-1 \quad 1]$ is a Zener–Stroh crack [20–25], which is a counterpart of the Griffith crack. Here we mention that the Griffith crack is an externally loaded crack while the Zener–Stroh crack is a net dislocation-loaded crack which is formed by a dislocation pileup. Interested readers may refer to more recent works [22–25] to find more detailed contents on Zener–Stroh crack. The sum of Burgers vectors of the dislocations insider the Zener–Stroh crack $[-1 \quad 1]$ is non-zero, more specifically

$$\int_{-1}^{1}[w_{,x}(x,0^-) - w_{,x}(x,0^+)]\mathrm{d}x = b_z. \tag{17}$$

In addition, no external mechanical loading is applied on the two-phase composite. The two analytic functions $f_1(\zeta)$ defined in the inhomogeneity and $f_2(\zeta)$ defined in the unbounded matrix can be expressed in closed-form as

$$\begin{aligned} f_1(\zeta) &= \frac{b_z}{2\pi}\Gamma \ln\zeta, \\ f_2(\zeta) &= \frac{b_z}{2\pi}\ln\zeta + \frac{b_z}{2\pi}(1-\Gamma)\left[\ln\left(\zeta - \frac{1}{c}\right) - \ln(\zeta - c)\right]. \end{aligned} \tag{18}$$

It is of interest to point out that the above two analytic functions for a Zener–Stroh crack can also be obtained from the previous solutions in Eq. (12) for a screw dislocation located in the matrix by letting the screw dislocation approach the crack face, i.e., $e = 1/\bar{e}$.

The stress field due to the Zener–Stroh crack is given by differentiating Eq. (18) as

$$\sigma_{zy} + \mathrm{i}\sigma_{zx} = \frac{\mu_1 \Gamma b_z \zeta}{\pi(\zeta^2 - 1)} \tag{19}$$

inside the inhomogeneity, and

$$\sigma_{zy} + \mathrm{i}\sigma_{zx} = \frac{\mu_2 b_z \zeta}{\pi(\zeta^2 - 1)} + \frac{\mu_2 (c^2 - 1)(\Gamma - 1) b_z \zeta^2}{\pi(\zeta^2 - 1)(c\zeta - 1)(\zeta - c)} \tag{20}$$

in the matrix. From the above expressions of stress field, we can arrive at the SIFs on the two tips of the crack as

$$\begin{aligned} K_{\mathrm{III}}^{\mathrm{L}} &= -\frac{\mu_2 b_z}{2\sqrt{\pi}}\left[1 + (1 - \Gamma)\frac{c - 1}{c + 1}\right], \\ K_{\mathrm{III}}^{\mathrm{R}} &= \frac{\mu_2 (2 - \Gamma) b_z}{2\sqrt{\pi}}, \end{aligned} \tag{21}$$

when $\mu_1 = \mu_2$, or $\Gamma = 1$, the above reduces to the results for a Zener–Stroh crack in a homogeneous material [24]. It is found from Eq. (21) that the SIF at the left tip is always negative, while the SIF at the right tip is always positive. In addition when the inhomogeneity is stiffer than the matrix, i.e., $\Gamma < 1$, then we have $|K_{\mathrm{III}}^{\mathrm{R}}| > |K_{\mathrm{III}}^{\mathrm{L}}| > \frac{\mu_2 b_z}{2\sqrt{\pi}}$; when the inhomogeneity is softer than the matrix, i.e., $\Gamma > 1$, then we have $|K_{\mathrm{III}}^{\mathrm{R}}| < |K_{\mathrm{III}}^{\mathrm{L}}| < \frac{\mu_2 b_z}{2\sqrt{\pi}}$. Here $\frac{\mu_2 b_z}{2\sqrt{\pi}}$ is the SIF for a Zener–Stroh crack of half-length 1 in a homogeneous elastic material with shear modulus μ_2. Fig. 8 illustrates the contour plots of the stress component σ_{zy} in the matrix with $c = 5$ and $\mu_1/\mu_2 = 2$. It is observed that the traction-free boundary condition on the crack surface is satisfied. We also notice that there exists a curve on which $\sigma_{zy} = 0$ besides the crack surface. σ_{zy} is negative on the left hand side of the curve, and it is positive on the right hand side of the curve. This curve is not the y-axis due to the existence of the inhomogeneity.

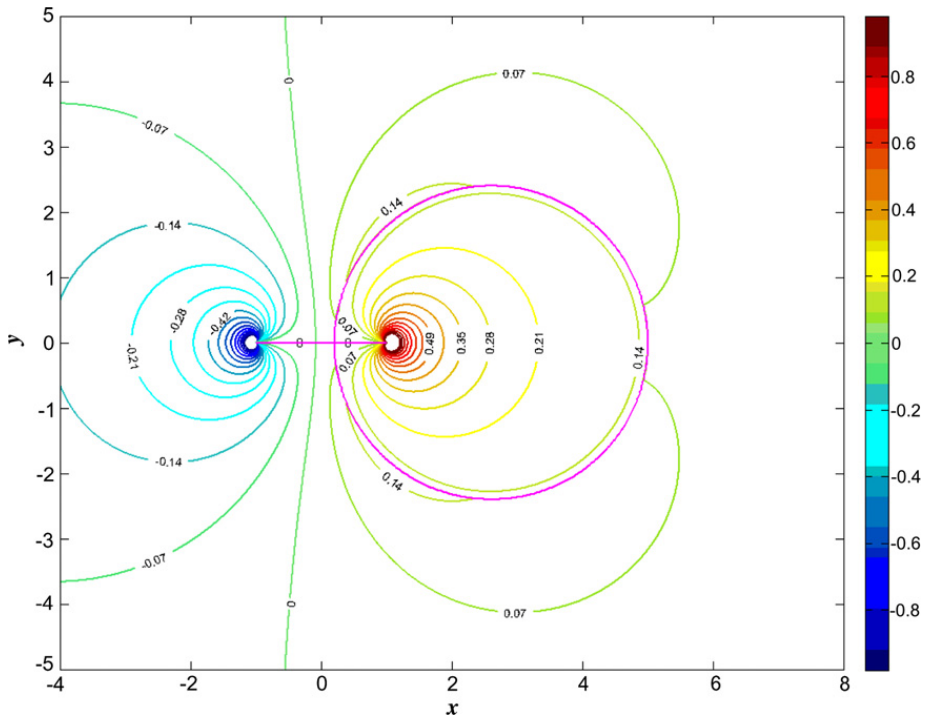

Fig. 8. Contours of the normalized stress component $\tilde{\sigma}_{zy} = \frac{\pi\sigma_{zy}}{\mu_2 b_z}$ with $c = 5$ and $\mu_1/\mu_2 = 2$. The crack $[-1 \quad 1]$ is a Zener–Stroh crack.

4. Conclusions

By means of conformal mapping (see Eq. (2)) and the method of image [8], closed-form solutions are derived for the elastostatic problem of a mode-III radial matrix crack penetrating a circular elastic inhomogeneity. Detailed results are given for three cases: (1) the two-phase composite is subjected to remote uniform antiplane shearing; (2) a screw dislocation is located in the matrix; (3) the radial crack is a Zener–Stroh crack. The case in which a screw dislocation lies within the inhomogeneity can be identically discussed. This investigation can also be considered as an extension of the results of Palaniappan [8] to the non-circular hybrid geometry case (here the slit crack is an extreme case of ellipse). While the present closed-form solutions can be utilized as a benchmark for future numerical study and meanwhile can be employed to investigate a cracked polycrystalline solid [6,7], we further expect that the present results can be extended to an arc shaped crack penetrating a circular inhomogeneity and can also be easily extended to a radial matrix crack penetrating a piezoelectric circular inhomogeneity.

Acknowledgement

The authors were greatly indebted to a referee for his/her very helpful comments and suggestions. This work was supported in part by AFOSR FA9550-06-1-0317.

Appendix

Let $\zeta \in C_b$, so we can write $\zeta = c + \sqrt{c^2 - 1}e^{i\theta}$. The inverse mapping of ζ in the original physical z-plane is

$$z = \frac{1}{2}(\zeta + \frac{1}{\zeta}) = \frac{1}{2}\left(c + \sqrt{c^2 - 1}e^{i\theta} + \frac{1}{c + \sqrt{c^2 - 1}e^{i\theta}}\right). \tag{A.1}$$

Then the following equality establishes

$$z - \frac{1}{2}\left(c + \frac{1}{c}\right) = \frac{1}{2}\left(c + \sqrt{c^2 - 1}e^{i\theta} + \frac{1}{c + \sqrt{c^2 - 1}e^{i\theta}}\right) - \frac{1}{2}\left(c + \frac{1}{c}\right) = \frac{1}{2}\left(c - \frac{1}{c}\right)\frac{\sqrt{c^2 - 1} + ce^{i\theta}}{\sqrt{c^2 - 1} + ce^{-i\theta}}. \tag{A.2}$$

As a result

$$\left|z - \frac{1}{2}\left(c + \frac{1}{c}\right)\right| = \frac{1}{2}\left(c - \frac{1}{c}\right), \tag{A.3}$$

which means that $z \in L$.

References

[1] F. Erdogan, G.D. Gupta, On the numerical solution of singular integral equations, Q. Appl. Math. 29 (1972) 525–534.
[2] F. Erdogan, G.D. Gupta, M. Ratawani, Interaction between a circular inclusion and an arbitrarily oriented crack, ASME J. Appl. Mech. 41 (1974) 1007–1013.
[3] H.A. Luo, Y. Chen, Matrix cracking in fiber-reinforced composite materials, ASME J. Appl. Mech. 58 (1991) 846–848.
[4] Z.M. Xiao, B.J. Chen, Stress intensity factor for a Griffith crack interacting with a coated inclusion, Int. J. Fract. 108 (2001) 193–205.
[5] X. Wang, Y.P. Shen, An edge dislocation in a three-phase composite cylinder model with a sliding interface, ASME J. Appl. Mech. 69 (2002) 527–538.
[6] Y.P. Wang, R. Ballarini, A long crack penetrating a circular inhomogeneity, Meccanica 38 (2003) 579–593.
[7] Y.P. Wang, R. Ballarini, A long crack penetrating a transforming inhomogeneity, ASME J. Appl. Mech. 71 (2004) 582–585.
[8] D. Palaniappan, Classical image treatment of a geometry composed of a circular conductor partially merged in a dielectric cylinder and related problems in electrostatics, J. Phys.: Math. Gen. 38 (2005) 6253–6269.
[9] W. Thomson (Lord Kelvin), Extrait D'une lettre de M. Liouville, Originally in J. Math. Pures Appl. 10 (1845) 364.
[10] E. Honein, T. Honein, G. Herrmann, On two circular inclusions in harmonic problems, Q. Appl. Math. 50 (1992) 479–499.
[11] D. Palaniappan, B.U. Felderholf, Electrostatics of the conducting double sphere, J. Appl. Phys. 86 (1999) 3418–3422.
[12] D. Palaniappan, Electrostatics of two intersecting conducting cylinders, Math. Comput. Modell. 36 (2002) 821–830.
[13] N.I. Muskhelishvili, Some Basic Problems of the Mathematical Theory of Elasticity, P. Noordhoff Ltd., Netherlands, 1963.
[14] J. Yoon, C.Q. Ru, A. Mioduchovski, Effect of a thin surface coating layer on thermal stresses within an elastic half-plane, Acta Mech. 185 (2006) 227–243.

[15] C.Q. Ru, P. Schiavone, A circular inclusion with circumferentially inhomogeneous interface in antiplane shear, Proc. R. Soc. Lond. A453 (1997) 2551–2572.
[16] F. Erdogan, A.C. Kaya, P.F. Joseph, The Mode-III crack problem in bonded materials with a nonhomogeneous interfacial zone, ASME J. Appl. Mech. 58 (1991) 419–427.
[17] S.D. Wang, S.B. Lee, Screw dislocation near a slant edge crack, Mech. Mater. 31 (1999) 63–70.
[18] B.T. Chen, C.T. Hu, S.B. Lee, The behavior of screw dislocations emitted from a star crack with a central hole, Int. J. Fract. 99 (1999) 293–306.
[19] X. Wang, Z. Zhong, A circular inclusion with a nonuniform interphase layer in antiplane shear, Int. J. Solids Struct. 40 (2003) 881–897.
[20] C. Zener, The Micro-Mechanism of Fracture. Fracturing of Metals, American Society for Metals, Cleveland, 1948, pp. 3–31.
[21] A.N. Stroh, The formation of cracks as a result of plastic flow, I, Proceedings of the Royal Society of London A 223 (1954) 404–414.
[22] Z.M. Xiao, B.J. Chen, H. Fan, A Zener–Stroh crack in a fiber-reinforced composite material, Mech. Mater. 32 (2000) 593–606.
[23] Z.M. Xiao, B.J. Chen, Stress analysis for a Zener–Stroh crack interacting with a coated inclusion, Int. J. Solids Struct. 38 (2001) 5007–5018.
[24] Z.M. Xiao, B.J. Chen, Electro-elastic stress analysis for a Zener–Stroh crack interacting with a coated inclusion in a piezoelectric solid, Acta Mech. 171 (2004) 29–40.
[25] Y.Z. Chen, X.Y. Lin, Singular integral equation method for multiple Zener–Stroh crack problems in antiplane elasticity, Eng. Anal. Bound. Elem. 31 (2007) 22–27.